Hindawi
Advances in Materials Science and Engineering
Volume 2022, Article ID 2165855, 16 pages
https://doi.org/10.1155/2022/2165855

Review Article

Effect of Nanomaterials on Tribological and Mechanical Properties of Polymer Nanocomposite Materials

M. S. Senthil Kumar,[1] Chithirai Pon Selvan,[2] K. Santhanam,[3] A. Kadirvel,[4] V. Chandraprabu ,[5] and L. SampathKumar[6]

[1]*Department of Mechanical Engineering, Builders Engineering College, Nathakadaiyur,Tirupur District, Kangeyam 638108, India*
[2]*Science and Engineering, Curtin University, Dubai International Academic City, Block 11,Fourth Floor,P. O. Box 345031, Dubai, UAE*
[3]*Department of Mechanical Engineering, K. S. Rangasamy College of Technology, Thokkavadi,Namakkal District, Tiruchengode 637215, India*
[4]*Department of Mechanical Engineering, R.M.K. Engineering College, Kavaraipettai, Gummidipoondi Taluk, Tiruvallur District 601 206, India*
[5]*School of Mechanical, Chemical & Materials Engineering, Adama Science & Technology University, Adama, Ethiopia*
[6]*Department of Physics, Builders Engineering College, Nathakadaiyur,Tirupur District, Kangeyam 638108, India*

Correspondence should be addressed to V. Chandraprabu; v.chandraprabu@astu.edu.et

Received 26 January 2022; Revised 3 April 2022; Accepted 4 April 2022; Published 31 May 2022

Academic Editor: Adam Khan M

The good adhesion and interfacial interaction between the nanomaterial and the matrix show that the low content polymer nanocomposite has better tribological and mechanical properties such as strength, modulus, fracture toughness, and fatigue properties. This phenomenon has attracted the attention of many researchers in this field for the past two decades. Nanomaterials are available in many forms, such as nanotubes, nanoclays, nanofibers, nanoparticles, and graphene depending on the shape. This article summarizes the mechanical test results of different nanocomposite materials under various operating conditions. In addition, the current research clearly describes various decisive factors that affect material properties, such as the dispersion of nanoparticles, clay tactoids, processing conditions, agglomeration, and distribution status. The tribological properties and fatigue resistance of nanocomposites are also discussed in this study. In addition, the article also discusses the related issues of incorporating nanomaterials into the matrix.

1. Introduction

Composite materials are used in various fields such as aerospace, automobiles, structural elements, construction, and sporting goods due to its high strength-to-weight ratio [1]. The rapid development of nanoscience makes it possible to clearly identify potential applications in many fields through continuous research. The main research on nanocomposites is obviously limited to two-phase nanocomposites (contains polymers modified by nanofillers), such as nanoclay/epoxy resin nanocomposites, but in some cases, researchers are studying three-phase composites (fiber reinforced with the nanofillers-modified polymers), such as nanoclay/epoxy/glass fiber nanocomposites to improve mechanical properties, as shown in Figure 1 [2].

Nowadays, some researchers have widely used various nanofillers in their research to improve the performance of composite materials as the performance of composite materials will increase significantly under low load on the matrix. The nanofiller contains at least one of the three external dimensions in the nanometer range of 1 nm or 10^{-3} μm or 10^{-9} m [3, 4]. Different types of thermoplastic

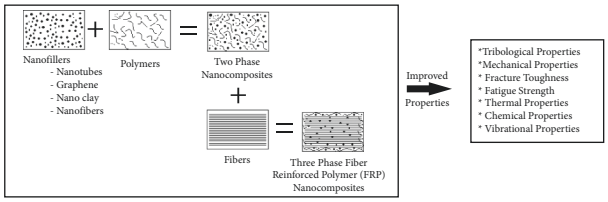

Figure 1: Scenario of property improvement by adding nanofillers with polymer and fiber.

and thermosetting polymer matrix like polyetherimide, polystyrene, polyester, epoxy, etc., are used to manufacture polymer matrix nanocomposite (PMNC) materials [5–8]. However, epoxy resin is a polymer matrix that is often used to make PMNC [9].

In general, depending upon the dimensions the nanofillers are classified as 1D (nanowires, nanorods, nanotubes, nanofibers), 2D (nanofilms, nanoplates, nanocoatings), and 3D (nanoparticles) [10, 11]. It is understood that carbon nanotubes (CNTs), halloysite nanotubes (HNTs), carbon nanofibers (CNFs) are the examples of 1D fibrous materials [8, 12–14]. Further, the 2D nanoclay contains a plate-like structure that has four groups such as smectite, illite, vermiculite, and kaolin-serpentine, and contains a high aspect ratio (30–1000) [6, 15]. Likewise, carbon black (CB), silica particles, fullerene, silica oxide, and titanium oxide are examples of 3D nanoparticles [12, 16].

Generally, the polymer matrix and the nanofiller are appropriately mixed through various methods, such as in-situ embedding polymerization, melt intercalation, polymer-particle direct mixing, in-situ polymerization, and sol-gel process [7, 17, 18]. However, among these various methods, the common methods for preparing polymer/nanomaterial mixtures are solution intercalation method, in-situ intercalation polymerization method, melt intercalation method, and direct in-situ synthesis method [19–23].

Based on the type and size of nanofiller, surface, aspect ratio, volume fraction, mixing method of polymer and nanofillers, operating parameters of mixing method, and the degree of mixing, researchers categorized four types of dispersions, namely, (1) phase separated or tactoid, (2) intercalated, (3) intercalated disordered, and (4) exfoliated [7, 8, 18, 24, 25]. In fact, the functioning of nanocomposites depends on the dispersion speed.

X-ray diffraction (XRD) and electron microscopy data confirmed the structure of the dispersed nano-filled polymer [8, 26]. Various researchers have shown that poor dispersion of the nanofiller/polymer mixture can cause agglomeration or factors in the matrix during their morphological studies. Using the method of nanocomposite materials, researchers found that the performance of nanocomposite materials will be reduced due to agglomeration. They also found that the lump formed led to a low degree of cross-linking of the filler matrix; however, with all the higher loads on the nanomaterials, agglomeration was inevitable [27–30].

The different varieties of agglomeration models were suggested by many researchers. The initial micromechanics model was developed by Shi et al. to study the waviness or curviness effect of carbon nanotubes [31]. Similarly, a lot of models were suggested by various researchers, for instance, the two-scale composite model and effective-medium theory used to predict the impact of graphene on the percolation threshold and overall conductivity [32, 33], micromechanics model to ascertain the coefficients of nonlinear thermal expansion of FRP laminates [34], a two-scale micromechanical model used to know the impact of nanotube collection and interface condition [35], Mori–Tanaka micromechanics method used to find the effect of elastic moduli [36], and Halpin–Tsai analytical models to find the effect of nanofiller loading on the thermal conductivity [37, 38].

In fact, the greater mechanical and thermal properties [25, 28–30], enhanced tribological properties [16, 39], superior morphological properties [7, 30], better dielectric properties [8, 32], increased vibration properties [26, 40], revised fatigue properties [41, 42], and commanding fracture toughness [43, 44] were attained for nanocomposites at low nanofiller loadings due to adhesion at the interface. Moreover, the interlaminar shear strength (ILSS) also increased greatly for the nanocomposites.

Mazumdar identified different manufacturing methods of the composite laminates like wet lay-up technique, pultrusion technique, resin transfer molding (RTM) process, vacuum-assisted resin transfer molding (VARTM) process, autoclave method, resin film infusion (RFI) process, prepreg technique, filament winding method, and fiber placement technique. Further, the researcher addressed that the degree of interaction between matrix and fiber is based upon the manufacturing methods. However, each method has certain disadvantages besides its advantages, for instance, void presence in wet lay-up technique, material accumulation at die in pultrusion technique, resin flow issue in RTM process, presence of dry spots in VARTM process, and higher fabrication in autoclave technique [45].

The current review provides detailed information about the effect of nanofiller reinforcements in nanocomposites on processing techniques of nanofiller/polymer blends, structure formation, manufacturing technique, characterization of nanocomposites, comparison of material properties with neat composites, and processability issues of nanocomposites. Moreover, this attempt would certainly attract both academic and industrial researchers in the field of nanocomposites.

2. Tribological Properties

Zhang et al. synthesized a nanocomposite with a Nomex fabric mixture filled with Polyfluo 150 wax (PFW) and nano-SiO_2. Nomex fibers were initially coated with phenolic resin. Tribological effects indicate that the inclusion of Polyfluo 150 wax and nanoparticles preferentially causes wear and reduced coefficient of friction (COF) for laminates. This development improved the tribological properties such as anti-wear and friction-reducing capabilities of nanocomposites. Furthermore, the optimum content of nano-SiO_2 in Nomex fabric composites revised the tribology property considerably [46]. With the assist of the Hysitron

Tribo Indenter system, Gu et al. performed the micro/nanoscale indentation and scratch tests on epoxy/silica nanocomposites coatings. The test results revealed that the silica particles decreased the friction coefficient and scratch depth [47]. In an another friction and wear research, the tribological properties of the nanocoatings were examined. The coatings were constructed from the blend of hydrophilic nano-silica particles and epoxy resin. From the test results, it is clear that the nano-silica particle interestingly altered the tribological properties. Additionally, the filler-loaded coatings significantly improved the surface roughness and water contact angle characteristics than the base epoxy coating [48].

The study by Thakur and Chauhan [49] portrayed the tribological properties of vinyl ester nanocomposites loaded with three different equally sized micron and submicron cenosphere particles with a diameter 400 nm, 900 nm, and 2 μm. The research was carried out using the Taguchi design technique as the design of experiments (DOE). The Taguchi design was created with an L_{27} (36) orthogonal array which includes six factors and three different levels as shown below. Finally, analysis of variance (ANOVA) was used in order to evaluate the impact of parameters on the COF and sliding wear resistance at the dry sliding conditions.

Factors and levels of variables in the DOE:

(A) Load (N) (level 1:10, level 2:40, level 3:70)

(B) Filler size (mm) (level 1:2, level 2:0.9, level 3:0.4)

(C) Filler content (%) (level 1:2, level 2:6, level 3:10)

(D) Roughness (mm) (level 1:0.02, level 2:0.2, level 3:0.7)

(E) Sliding speed (m/s) (level 1:1.3, level 2:3.2, level 3: 5.7)

(F) Sliding distance (m) (level 1:2000, level 2:4000, level 3:6000)

The tribological test found out that the wear properties of the submicron size filler particles contribute notably by 21.18% and 11.58% better than that of the micro-sized particles. The DOE corroborates the load, and particle content had been the essential constraints among the other factors which influenced the COF by 68.33% and 9.81% and wear resistance by 63.89% and 13.39%. In general, the wear properties of laminates had elevated with increasing content of the cenosphere. Microscopic observations of the worn surfaces demonstrated that the superior properties are achieved to 400 nm cenosphere particles-filled vinyl ester composite due to the uniform and robust adhesion to the counterface. Further, the result portrayed that the significant wear resistance occurred to the 6 wt.% nanoparticles-filled composites. The major wear in the mechanism of panels is exchanged from the hard abrasive wear to moderate abrasive wear.

The research of Akil et al. targeted on finding the impact of two different filler reinforcements: one is particulate (talc particles of an average particle size less than 45 μm), and another one is fiber (chopped strands E-glass fiber) composites on the wear and friction properties. The panels contain GUR 4120 grade ultra-high molecular weight polyethylene (UHMWPE) modified with 100 nm size zinc oxide (ZnO) nanofillers with 10 wt.%. The nanocomposite was fabricated in the hot compression molding machine. The entire tribological study was tested in a pin-on-disk testing machine based on the response of the surface Box–Behnken design (BBD) which is shown in Figure 2. The different input variables were applied load, sliding speed, and sliding distance. Basically, BBD is an experimental design for response surface methodology which does not include embedded factorial or fractional factorial design. It requires three levels of each factor. The design uses 12 middle edge positions and three center positions [50].

The input variables were placed as shown below at one of three equally spaced values, usually as −1, 0, and +1(minimum, center, and maximum), statistically generated by the MINITAB 16 software. The impact of input variables on the wear loss and the average COF of hybrid composites were analyzed by the response surface methodology method. The ANOVA was conducted with a confidence level of 95% on each model. The mathematical models showcased that the input variables significantly affect the tribological properties of composites under the given range of variables. The compounded effects of load and sliding distance greatly influenced on the wear loss and COF for both hybrid composites. The glass fiber-reinforced laminates have shown superior wear properties and less severity of worn-out surfaces than the talc-reinforced laminates.

Independent variables and variation levels of the BBD:

(X1) Applied load (N) (variation level −1: 9.81, variation level 0: 19.62, variation level 1: 29.43)

(X2) Sliding speed (m/s) (variation level −1: 0.2094, variation level 0: 0.4188, variation level 1: 0.6282)

(X3) Sliding distance (m) (variation level −1: 125.64, variation level 0: 251.28, variation level 1: 376.92)

In another study, Akil et al. investigated the tribological performances of ZnO nanoparticles-reinforced UHMWPE composite and demonstrated the response of filler loadings from 5 to 20 wt.%. The wear test was carried out in dry sliding situations with load varying between 5 and 35 N, and sliding speed varying between 0.209 m/s to 0.419 m/s in opposition to the silicon carbide abrasive paper. Wear resistance significantly stepped forward at 10 wt.% ZnO/UHMWPE nanocomposite. The average coefficient of friction of the UHMWPE composite showed a downward fashion while reinforcing with ZnO nanoparticles. Further, the severity of wear of the worn surface was found to be decreased due to the ZnO nanoparticle reinforcement [51].

Louis Winnubst et al. inspected the friction and wear properties of nanocomposites, made up through the compression molding consisting of silica (SiO_2) particles of nanometer-sized blended in the nylon-6 polymer. During the test, in the pin-on-disk test, the flat pin made up of steel was running toward a composite disk. Compared with pure nylon 6, adding 2% by weight of SiO_2 particles can reduce friction by 0.5–0.18. As a result, the low silica content reduced the wear rate by 140 times. The adhesion and interlocking of material into metal asperities have developed

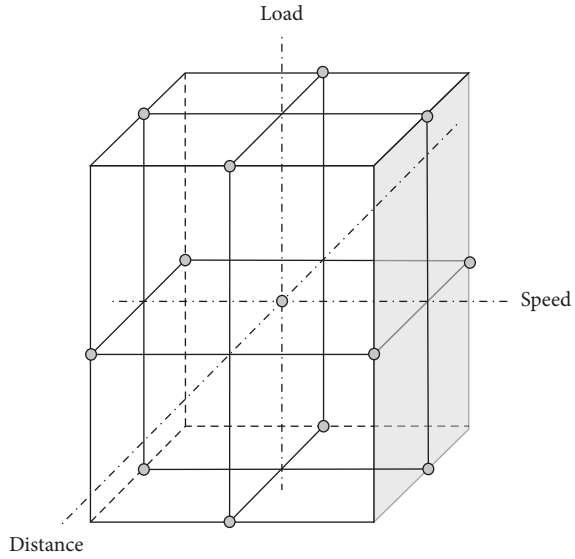

Figure 2: Box–Behnken design.

a transfer film over the steel pin. In addition, the test revealed two phenomena. First, the wear is based on the adhesion between the transfer film and the contact surface. The second is to use a transfer film to protect the polymer surface from metal roughness [52]. Similarly, a wear resistance study on the effect of SiC particles in laminated polyimide/SiC laminates obtained by hot dynamic compaction method confirmed that the abrasive and delamination were the dominant factors in wear mechanisms. In addition, the wear resistance of the samples filled with SiC nanoparticles decreases significantly with the increase in the number of SiC particles [16].

3. Tensile Strength

Qi et al. evaluated the material changes of nanocomposites that were prepared with the help of in-situ polymerization technique by including four types of montmorillonite (MMT) nanoclays, such as pristine (Na^+), Cloisite 30B (C30B), cetylpyridinium chloride (CPC), and Nanomer I.30E (NI.30E) in the base epoxy resin. The modulus of elasticity and fracture toughness are significantly improved [53]. In addition, as the load on the nanoclay increases, the tensile strength and deformation decrease significantly, as shown in Table 1. The declined trend could occur because of the improper dispersion rate of nanofillers in the matrix, which led to a high-stress concentration.

The researchers have dispersed different nanoclays in both thermoset and thermoplastic resins, for instance, Cloisite 15A, Cloisite 93A, and Cloisite Na dispersed with vinyl ester matrix by using ultrasonicator and twin-screw extruder [58], and Cloisite 30B and Cloisite 25A clays mixed with three resins diglycidyl ether of bisphenol A (DGEBA), hexanediol diglycidyl ether (HDE), and diglycidyl ether of bisphenol F (DGEBF) with the help of ultrasonicator [59]. Similarly, Cloisite Na+ and Cloisite 30B nanoclay content in epoxy [27] and Cloisite 25A nanoclay were dispersed with the aid of mechanical stirrer in epoxy resin [60]. Murthy et al. had obtained the tensile properties in the order of Cloisite 15A > Cloisite Na > Cloisite 93A [58]. Interestingly, Dorigatoa and Pegorettia detected the amplified tensile properties for smaller clay content [59]. Similarly, Basara et al. got better tensile properties for Cloisite 30B nanoclay at lower clay content than the Cloisite Na+ [27]. Contrarily, the authors notified the improved tensile modulus for both the nanoclays in increasing nanoclay content.

In another case, due to the presence of nanoclay, the analyst realized a reduction in the thermomechanical value [60]. The investigations of Panneerselvam and Daniel on polypropylene/Cloisite 15A nanocomposites and polymer matrix/spherical glass particle composites noticed a significant improvement in tensile strength for both materials [61]. However, when compared with nanocomposite materials, composite laminates have a commanding improvement in tensile strength.

Generally, carbon nanotubes (CNTs) are available in various forms like cup-stacked carbon nanotubes (CSCNTs), single-wall carbon nanotubes (SWCNTs), double-walled carbon nanotubes (DWCNTs), and multi-walled carbon nanotubes (MWCNTs). When CSCNT and MWCNT are dispersed together with the matrix, the tensile strength performance of the nanocomposite laminate has shown significant development as in Table 1. The tensile properties were enhanced commandingly when carbon fibers, basalt fibers, and polyacrylonitrile-based T650 and IM-7 carbon fibers were reinforced with the CNTs-functionalized matrix [54, 55, 62]. Besides that, some researchers had used different nanoreinforcements to functionalize the epoxy resins like Somasif ME-100 layered silicate [57] and nanocalcium carbonate (nano-$CaCO_3$) [63]. Table 1 expresses the experimental results of Kornmann et al. that the 10 wt.% nanocomposites were superior to the neat laminates. In a similar way, carbon fibers and carbon nanofibers are used to improve tensile properties by directly embedding them in a pure matrix or a matrix loaded with nanofillers [63–65].

Interestingly, Baur et al. directly grew multi-walled carbon nanotubes (MWCNTs) on two different polyacrylonitrile-based carbon fibers during the thermal chemical vapor deposition process [62]. As shown in Figure 3, the mixture of ferrocene/xylene vapor, argon, and hydrogen is heated from 700°C to 800°C in a quartz glass tube. Finally, CNTs were grown on the carbon fiber substrate inside the tube. The author studied in detail the chemical vapor deposition (CVD) growth conditions of individual fibers and the influence of MWCNT morphology. The tensile strength of the hybrid fiber depends on the type, size, or coating of the carbon fiber, temperature and growth time, and atmospheric conditions in the tube. In addition, the tensile strength of the sized carbon fiber decreases, in the initial stage of the carbon nanotube growth process. This phenomenon is due to the lack of organic materials at the growth temperature, leading to mechanical defects.

4. Flexural Strength

Manfredi et al. produced three E-type glass fiber-reinforced nanocomposites by adding 3 wt.% and 5 wt.% of Cloisite 30B, and 3 wt.% of Cloisite 10A nanoclays to the base matrix

Table 1: Tensile testing results of different nanocomposites.

Nanocomposites	Young's modulus (GPa)	Tensile strength (MPa)	Ref.
Neat DGEBA epoxy	2.71 ± 0.11	72.06 ± 1.37	[53]
2 wt.% Na+/DGEBA epoxy	2.79 ± 0.07	68.04 ± 4	[53]
5 wt.% Na+/DGEBA epoxy	2.92 ± 0.17	57.2 ± 2.22	[53]
10 wt.% Na+/DGEBA epoxy	3.44 ± 0.29	57.68 ± 3.69	[53]
2 wt.% C30B/DGEBA epoxy	3.11 ± 0.09	62.19 ± 2.56	[53]
5 wt.% C30B/DGEBA epoxy	3.10 ± 0.08	58.35 ± 5.87	[53]
10 wt.% C30B/DGEBA epoxy	3.12 ± 0.23	57.31 ± 6.97	[53]
2 wt.% NI.30E/DGEBA epoxy	2.68 ± 0.26	64.58 ± 6.56	[53]
5 wt.% NI.30E/DGEBA epoxy	2.82 ± 0.12	59.94 ± 9.01	[53]
10 wt.% NI.30E/DGEBA epoxy	3.04 ± 0.11	58.23 ± 4.39	[53]
2 wt.% CPC/DGEBA epoxy	2.57 ± 0.15	49.03 ± 2.72	[53]
5 wt.% CPC/DGEBA epoxy	2.79 ± 0.08	50.14 ± 2.80	[53]
Neat DGEBA epoxy/carbon fiber	46.5 ± 0.6	848 ± 18.2	[54]
5 wt.% CSCNT/DGEBA epoxy/carbon fiber	47.9 ± 0.7	844 ± 5.3	[54]
10 wt.% CSCNT/DGEBA epoxy/carbon fiber	48.3 ± 1.7	850 ± 40.0	[54]
Neat DGEBA epoxy/basalt fiber	27.65 ± 0.41	584.7 ± 10.3	[55]
0.5 wt.% raw MWCNT/DGEBA epoxy/basalt fiber	27.44 ± 0.76	564.0 ± 31.0	[55]
0.5 wt.% o-MWCNT(acid treated)/DGEBA epoxy/basalt fiber	30.41 ± 1.31	635.7 ± 33.8	[55]
0.5 wt.% PGE-MWCNT(phenyl glycidyl ether added)/DGEBA epoxy/basalt fiber	29.92 ± 0.83	608.8 ± 20.0	[55]
1.5 wt.% raw MWCNT/DGEBA epoxy/basalt fiber	28.53 ± 1.18	504.0 ± 42.0	[55]
1.5 wt.% o-MWCNT/DGEBA epoxy/basalt fiber	36.4 ± 0.97	627.7 ± 25.5	[55]
1.5 wt.% PGE-MWCNT/DGEBA epoxy/basalt fiber	34.90 ± 0.77	615.1 ± 19.7	[55]
1.25 wt.% attapulgite clay(ATT)/DGEBA epoxy/basalt fiber	29.85 ± 1.03	530.9 ± 43.4	[55]
2.5 wt.% ATT/DGEBA epoxy/basalt fiber	28.06 ± 2.62	465.4 ± 94.5	[55]
Neat poly(ethylene terephthalate) (PET) polyclear-machine direction (MD)	2.0 ± 0.1	62.6 ± 0.7	[56]
1 wt.% MWCNT/PET-MD	2.25 ± 0.07	66.9 ± 0.8	[56]
2 wt.% MWCNT/PET- MD	2.57 ± 0.08	72.5 ± 0.2	[56]
4 wt.% MWCNT/PET- MD	2.80 ± 0.32	89.1 ± 4.2	[56]
Neat PET-transverse direction (TD)	1.93 ± 0.01	59.0 ± 1.2	[56]
1 wt.% MWCNT/PET- TD	2.13 ± 0.08	65.4 ± 0.7	[56]
2 wt.% MWCNT/PET- TD	2.34 ± 0.20	68.2 ± 1.0	[56]
4 wt.% MWCNT/PET- TD	2.75 ± 0.08	76.5 ± 0.8	[56]
Neat DGEBA epoxy	3062 ± 47	80.3 ± 0.8	[57]
10 wt.% Somasif M-100/DGEBA epoxy	4719 ± 130	51.5 ± 1.4	[57]

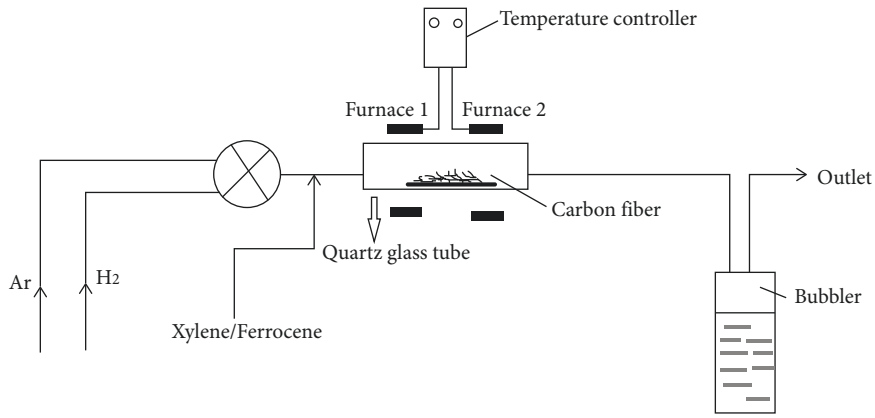

Figure 3: Schematic illustration for the development of CNT on the CF.

(epoxy resin) [66]. The mechanical properties, ILSS, and glass transition temperature were evaluated before and after immersing the sample in water. The study exposed that the higher flexural modulus and flexural strength have attained at 3 wt.% Cloisite 10A and 5 wt.% Cloisite 10A loaded glass fiber-reinforced polymer (GFRP) laminates, respectively. Through the water absorption test, the authors identified that the Cloisite 10A nanocomposites hold the less hydrophilic modifier, due to its superior flexural properties than the others. Furthermore, it was found that the reduced cross-linking density of the nanoclay results in absorbing more water than neat epoxy.

Hossain et al. had prepared the E-glass fiber-reinforced nanocomposites by VARTM machine by modifying the polyester resin with carbon nanofibers [67]. The flexural test on laminates revealed that commanding improvement on flexural strength and modulus was attained in nanocomposites than glass fiber-reinforced conventional composites. Karippal et al. had used Nanomer 1.30E nanoclay in the range of 0–6 wt.% to prepare epoxy/glass/nanoclay hybrid nanocomposite laminates through the use of the hand lay-up technique [25]. Based on the experimental results, the researchers concluded that the higher flexural properties were attained because of the best dispersion of 5 wt.% nanoclay in the base matrix. In the same manner, Sharma et al. synthesized Cloisite 30B (1, 3, and 5 wt.%)/epoxy resin/E-glass unidirectional fiber-reinforced nanocomposite laminates with the aid of using the usage of the hand lay-up method. Authors attained the commanding flexural strength for 5 wt.% clay loading GFRP laminates [68]. Again, the same trend was attained using 5 wt.% CNF-loaded carbon fiber/CNF/matrix nanocomposites. This trend took place because of the lesser open and closed porosity on the interface [69].

Alireza Ashori et al. analyzed the characteristics of wood-plastic composite (WPC) panels made of medium-density fiberboard and Cloisite 15A nanoclay residue sanding dust (SD). The polypropylene pellets, maleate-grafted polypropylene, SD, and nanoclay blends are first added in different proportions, and then the blends are directly fed into the counter-rotating twin-screw extruder. All the extruded filaments were pelletized by passing through a water bath, and finally, the pellets are placed in a hot press and made into a laminate. The flexural test shows that SD and nanoclay have achieved exceptional results in the flexural properties of the WPCs. By adding 2 wt.% of Cloisite 15A nanoclay to the matrix, the flexural strength is significantly improved, but the flexural properties are significantly reduced at 4% and 6% by weight. In contrast, due to the reduced adhesion in the fiber-matrix interface, the flexural properties of the laminate after the addition of SD are significantly reduced [70]. The flexural strength of polyamide 66/polypropylene (PA66/PP) mixture, graphite (Gr)-introduced PA66/PP, nanoclay-introduced PA66/PP, and short carbon fiber (SCF)-reinforced nanoclay-introduced PA66/PP laminates were studied. All composite panels use twin-screw extruder and injection molding. Experimental analysis shows that the presence of 2 wt.% nanoclay and 10% SCF increases the flexural strength and flexural modulus of the PA66/PP blend to 52 MPa and 1010 MPa, respectively [71].

In addition, electrospun polyether ketone nanofibers are applied to carbon fabrics to improve the flexural property of nanocomposites. In the course of their work, the researchers found that thinner nanofibers have higher bending properties, but as the thickness of the interlayer of nanofibers increases, these properties deteriorate [72]. Researchers added a small amount (0.25 wt.%) of electrospun glass nanofibers (EGNFs) to the epoxy resin/glass microfiber-reinforced hybrid nanocomposite made by the VARTM process, as shown in Figure 4, and achieved significant improvement in flexural properties. Xu and Hoa used hot melt lay-up and autoclave techniques to study the flexural properties of carbon fiber/epoxy/clay nanocomposite laminates [73]. The composite material made of carbon fiber-reinforced polymer (CFRP) has achieved a significant increase in flexural strength with 2 phr nanoclay loaded.

5. Compression Strength

Carbon nanofiber-reinforced hierarchical nanocomposites with multi-scale reinforcement fabrics have been synthesized in two stages by Minai et al. First, a multi-scale reinforced fabric (MRF) is synthesized by electrophoretic deposition of carboxylic acid or amine-functionalized CNF on the surface of a sized or unsized carbon fiber layer in an aqueous medium. In the next step, the MRF is placed first, and then the epoxy-amine resin mixture is poured into the resulting preform using a vacuum-assisted resin transfer molding machine. The superior compressive strength is attained to the resulting hierarchical nanocomposites with the amine-functionalized CNFs [74].

Uddin and Sun used nano-silica particles to modify DGEBA epoxy resin and developed a nano-silica/unidirectional glass fiber/epoxy laminate [75]. The uniform distribution of nano-silica particles in the epoxy resin significantly improves the longitudinal compressive strength. In addition, by incorporating nano-silica particles into epoxy resin, Manjunatha et al. [76] have achieved an equivalent increase in compressive strength. In their research, the authors used GFR nanocomposite laminates made by resin infusion under flexible tooling. Further, the compression test was carried out by Yokozeki et al. and proved evidence that there are no global buckling and no visible damage. As seen, Table 2 highlights the trend of increasing compressive strength of the CSCNT/epoxy/carbon fiber nanocomposites with respect to growing CNT content material due to commanding stiffness [51].

Arun and Sun used TEM instruments to observe the introduction of resin between the gallery spaces of Nanomer clay with a few exfoliated regions. In addition, the SEM image shows the presence of double platelets in better clay inclusion. This phenomenon will affect the longitudinal compression strength (off-axis) of the higher clay-loaded samples produced by the vacuum-assisted wet lay-up process. The self-adjusting mechanism is used for off-axis compression testing. During the test, the bending moment was eliminated by the complete contact between the load surface and the cemented carbide block. In the case of fiber composites modified with nanoclay, the compressive strength is increased by about 22%. The elastoplastic model created by the researchers confirmed the same trend [77]. In another study, Yutaka et al. performed static compression tests on two-phase nanocomposites and three-phase nanocomposites [78]. Cup-stack carbon nanofiber (CSNF) and CSNT/carbon nanofibers/resin are added to the resin to make two-phase and three-phase nanocomposites. The two-phase specimens are compressed in between the two hydraulic grips of the testing machine as shown in Figure 5(a) and the three-phase specimens were compressed by hydraulic grips as shown in Figure 5(b).

The authors found that the compressive properties of two-phase and three-phase laminates have improved.

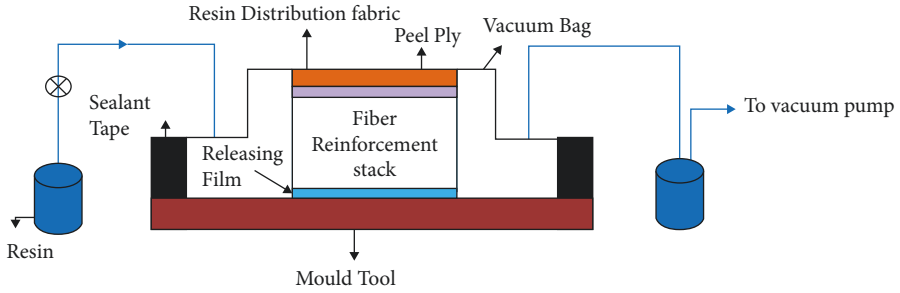

Figure 4: The schematic diagram of VARTM.

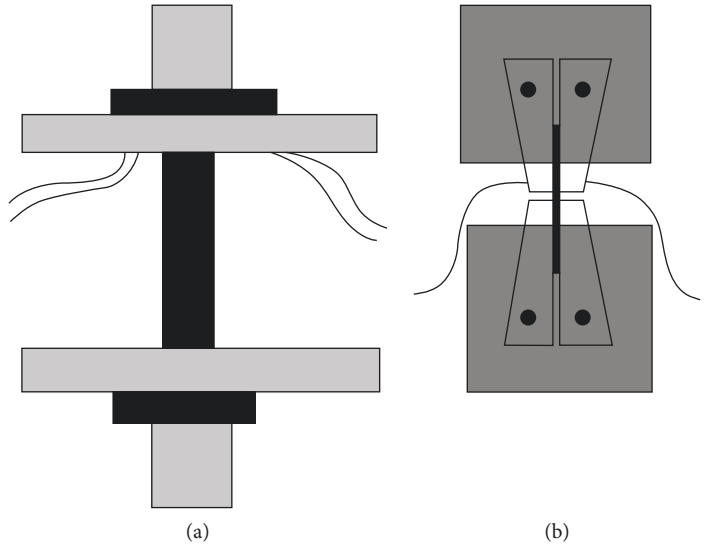

Figure 5: The schematic diagram of compressive modulus test: (a) two-phase composite and (b) three-phase composite.

Table 2: Summary of compression experimental results.

	0 wt.%	5 wt.%	10 wt.%
Compressive modulus (GPa)	42.9 (1.6)	43.2 (1.5)	45.1 (1.5)
Compressive strength (MPa)	488 (16.6)	501 (25.8)	539 (26.8)

However, they did not observe a monotonous relationship between the CSNF filler content and the compression properties of the three-phase composites. Surprisingly, better nanofillers provide excellent two-phase bond strength by weight. MWCNT/epoxy nanocomposite also has the same trend. Regardless of the technical strategy used to manufacture nanocomposites, higher concentrations of reinforcing fillers can provide superior compressive strength [79]. In contrast, the higher Nanomer I.28 nanoclay content in the matrix leads to a decrease in compressive strength due to the subtle interfacial adhesion between the clay and the base resin and the existence of nanovoids [80].

6. Fatigue Strength

Sumfleth et al. carried out each static and dynamic fatigue test to discover the fatigue property of glass fiber-reinforced (GFR) epoxy resin composites changed with a low quantity of fumed silica particles and MWCNT [81]. The dynamic fatigue test results confirmed that the inclusion of nanoparticles enhanced the inter-fiber fracture strength and leads to improved fatigue properties in high cycle fatigue. Similarly, Zhou et al. studied the fatigue performances of carbon nanofiber/epoxy/carbon fiber laminates [82]. During the investigation, the uniform mixture between the epoxy resin and CNF was acquired with the aid of a high-intensity ultrasonic liquid processor and an excessive pace mechanical agitator. The experimental results revealed that the 2 wt.% CNF-filled matrix possessed the highest fatigue strength. The researchers further fabricated the 2 wt.% CNF-modified epoxy/satin carbon fabric-reinforced nanocomposite panels in a VARTM machine. The fatigue test results of nanofiller-filled CFRP laminates revealed a commanding development than neat CFRP laminates.

Manjunatha et al. produced two kinds of GFRP composites neat epoxy (GFRP-neat) and hybrid particle-modified epoxy (GFRP-hybrid) using resin infusion method under flexible tooling setup. The hybrid particles which were used to modify the resin contain 9 wt.% of carboxyl-terminated butadiene-acrylonitrile (CTBN) rubber microparticles and 10 wt.% of silica nanoparticles [41, 42, 68, 83, 84]. The fatigue test was carried out according to the WISPERX load sequence for both GFRP-neat and GFRP-hybrid laminates. The test results seem to reflect the fatigue life of the

nanocomposite. Due to the suppression of matrix cracks and the reduction in the growth rate of delamination, the fatigue performance of the GFRP-hybrid laminate is 4 to 5 times higher than that of the GFRP-neat laminate. For all stress ratios of tension-tension, tension-compression, and compression-compression sections, both the laminates achieve constant amplitude fatigue life. In addition, it was found that the fatigue life calculated from the WISPERX load spectrum was significantly correlated with the experimental observations of both GRP laminates [41]. The author studied the similar fatigue behavior of GFRP-neat and the GFRP-hybrid epoxy laminates with a stress coefficient of $R = 0.1$. As in the previous case, researchers attained 6 to 10 times longer fatigue life for GFRP-hybrid epoxy composite laminates. This is achieved by suppressed matrix cracking and reduced cracking propagation in the particles-filled epoxy. This phenomenon is caused by the mechanism of cavitation, plastic deformation of rubber particles, and the growth of plastic cavities due to the fragmentation of silica particles [83]. The researchers studied the fatigue life of GFRP-neat and the GFRP-hybrid epoxy laminates under three different amplitude loading sequences, namely, three-step increasing block, three-step decreasing block, and random block load sequence. Due to the fracture of the matrix and the decrease in stiffness, the fatigue life of the GFRP-hybrid laminate is achieved in all load sequences with variable amplitudes [84].

7. Fracture Toughness

Nowadays, in industries, the thermoset polymer is widely used to create engineering components than the thermoplastic polymer on account of its appreciable mechanical properties. For the most part, the thermoset polymers are brittle in nature and exposed to crack. But, this property can be modified by including appropriate micro-sized or nano-sized particles in the base matrix. The current review by Lee et al. attempts to improve the fracture toughness of thermoset polymers by adding nano-sized conductive carbon black particles and Cloisite 93A nanoclay in the epoxy resin [85]. The procedure for mixing nanoparticles in the matrix contains three steps. First, mix the nanofiller with the epoxy resin by hand, and then mix it with a magnetic stirrer at 60°C for 60 minutes. Second, the mixture is added to the three rolls through the hopper for high shear mixing. Finally, use a magnetic stirrer to thoroughly mix the slurry and hardener under vacuum.

The fracture toughness test was performed at room temperature and cryogenic temperature. The test revealed that in room temperature the nanofillers notably improved the toughness than in the cryogenic temperature. Phonthammachai et al. stepped forward the overall performance of multilayer CFRP laminates with the aid of using unmodified nanoclay in epoxy [54]. The addition of 0.6 vol.% clay significantly improved the viscosity of the resin. The improved properties of resin brought improved toughness of cured nanocomposites. Martín-Martínez et al. [86] fabricated the laminates by adding high-performance clay in unsaturated polyester resin (UPR) coating on brown emperor natural stone and studied the fracture toughness properties. At the end of the study, it had been ascertained that the nanocomposites with a low clay content of 0.5 and 1 wt.% clay improved the fracture toughness significantly due to decreased gel time and decreased shrinkage degree of the UPR base matrix during curing. Kim et al. examined the mode I interlaminar fracture behavior of carbon fiber/nanoclay/epoxy matrix with the assist of a double cantilever beam (DCB) test setup [87]. The dimensions and preliminary crack size with Teflon film of DCB specimen are depicted in Figure 6. A good bonding was formed between the toughness of the clay-filled matrix and carbon fiber. Therefore, the fracture toughness property of laminates improved with increasing clay content during initiation and propagation stages. Especially, the propagation of crack was almost doubled for 7 wt.% nanofiller loadings. Likewise, the same trend was continued to nanocomposites which are manufactured by the vacuum infusion method with woven glass fabrics and clay-filled matrix [88].

The mode I (G_{Ic}) and mode II (G_{IIc}) fracture toughness of carbon fiber-reinforced laminates made of epoxy-filled nano-silica particles was studied. The epoxy resin contains 10% and 20% by weight of nanoparticles. The G_{Ic} improved when nano-silica loadings in resins were increased. On the contrary, G_{IIc} decreased with increasing nano-silica content. Similar research was carried out in CNT/epoxy/carbon fiber laminates. The G_{IIc} and G_{Ic} decreased considerably to silica nanoparticles-filled laminates than CNT-filled laminates. Further, from the fractographic study, it was evident that more interfacial failure happened between epoxy and CF particularly at higher loading for nano-silica particles-loaded laminates [89]. Davis and Whelan had conducted an experimental study on fracture toughness to CFRP laminates made by using fluorine-functionalized carbon nanotubes (f-CNTs)-modified epoxy. First, the f-CNT is applied to the center plane of the carbon fiber fabric of the laminate, thereby achieving a very good interlayer thickness enhancement. Davis and Whelan used four-point end notch flexure (4ENF) test setup to examine the critical strain energy release rate of nanocomposites. Figure 7 shows the 4ENF sample loaded in the four-point bend loading mode. Due to the strong covalent bond between carbon fiber and polymer resin, the use of 0.5 wt.% f-CNTs-loaded fabric resulted in an unexpectedly significant improvement in toughness. The covalent bond leads to an increase in the interface resistance between the fiber and the matrix [90]. In addition, Chan et al. studied the fracture toughness properties of nanocomposites made of carbon fiber reinforced by halloysite nanotubes in a hardened epoxy resin matrix. The toughness properties of the panel were calculated by using a double cantilever beam (DCB) test setup to conduct mode I and mode II fracture toughness tests. The test results show that due to the uniform distribution of HNT in the matrix, the participation of HNT in the panels significantly increases the fracture strength [91].

Kostopoulos et al. improved the toughness of CFRP by modifying CNF resin with piezoelectric particles (PZT). The experimental results show that when 1% by weight of CNF is introduced together with the matrix, the effect of CNF and resin leads to the bridging properties of the fiber, and a huge

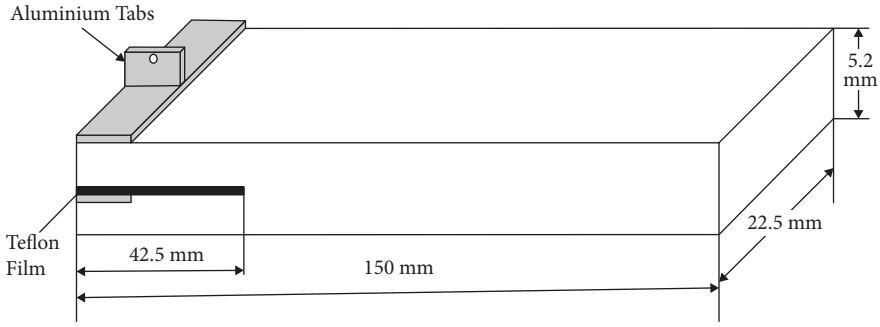

Figure 6: Geometry of DCB specimens.

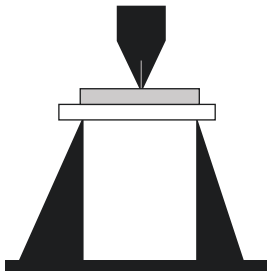

Figure 7: The schematic diagram of 4ENF specimen in a four-point bend mode.

Table 3: Effect of clay content on impact strength for nanocomposites.

Nanocomposites	Impact strength (J/m)
Neat TPO resin	80.00
5%Na-MMT/TPO resin	96.00
5%C20A/TPO resin	127.86
5%C30B/TPO resin	121.2
5%C20A5%COM/TPO resin	328.3
5%C30B5%COM/TPO resin	241.4

increase in the destruction energy of 100% is achieved. In contrast, due to the brittleness of particle inclusions, the addition of PZT particles results in lower fracture toughness [92]. Yao et al. synthesized the SiO_2 matrix nanocomposite using the sol-gel technique by magnetic force and ultrasonicator. The matrix contains a combination of three parts, namely, diglycidyl ether of bisphenol F (DGEBF), poly(-propylene glycol) diglycidyl ether (PPGDE), and diethyltoluene diamine (DETD). The mixture ratio of A and B parts is 1 : 1. The digital speckle correlation technique addressed that the distribution of displacement field in nanocomposites was happening at the initial edge crack tip. The three-point bending test results depicted that at low particle loading, the higher fracture toughness and larger deformation opposing capability were attained [93]. Ye et al. used 35 nm carbon black superconducting nanoparticles and a small amount of copper chloride (CC) as nanofillers and glass fibers for the manufacture of nanocomposites using vacuum resin infusion (VARI) technology. The electrical resistance tomography method was used to evaluate the transverse impact damage of laminates. This method is used to evaluate both damages such as in-plane and through-thickness directions of conductive points of GFRP laminates. This study investigated the improvement of G_{Ic} and G_{IIc} in laminates due to the presence of CB and CC nanoparticles. At the end of the test, delamination growth is characterized by changes in in-situ electrical resistance [94].

8. Impact Strength

The reason for this research was to ascertain the improvement of impact strength of laminates which are fabricated by polylactic acid filled with cellulose nanofiber and compatibilized with maleated PLA. The composite laminate was originally made by melt blending 5 wt.% maleated PLA and then using a twin-screw extruder to blend with two different nanofiber fillers, viz. 3 and 5 wt.%. The impact test shows that, compared with pure PLA, the addition of nanocellulose without maleated PLA will not significantly increase the impact strength of the laminate. Surprisingly, the results show that the 5 wt.% cellulose nanofiber-added nanocomposites have a significant increase in impact strength of 131% compared to pure PLA. This improvement is due to the uniform dispersion of CNF with the PLA matrix in the presence of maleated PLA [14]. In addition, compared with Cloisite Na + nanoclay, Basara et al. determined that Cloisite 30B nanoclay has higher impact strength because of the greater d-spacing at low clay content [27]. Similarly, due to the improved resin viscosity and lower resin shrinkage at curing, the commanding impact strength was achieved by adding 0.5 and 1% by weight of unmodified nanoclay in base matrix UPR [86].

Melt-extrusion nanocomposites contain three different montmorillonite nanoclays as reinforcing elements, namely, Cloisite Na-MMT, Cloisite 20A (C20A), and Cloisite 30B (C30B). The matrix contains thermoplastic polyolefin (TPO) resin and polypropylene grafted maleic anhydride (PP-g-MA) compatibilizer. Nanoclay is added in an amount of three percent, such as 3, 5, and 7 wt.% with the matrix. As shown in Table 3, the 5 wt.% C20A composites with 5 wt.% compatibilizer show better mechanical properties than other nanocomposites. The table clearly portrayed the improvement in impact strength of 5 wt.% C20A nanocomposites when compared to Na-MMT nanocomposites as 33% for C20A and 26% for C30B without compatibilizer due to the insertion of polymeric chain inside the clay platelet. But surprisingly, when adding 5% compatibilizer with the

composite, the IS increased to 242% for C20A and 151% for C30B due to the appreciable reinforcing effect made between clay and polymer.

Lou et al. conducted a detailed study to determine the impact strength (IS) of pure polyamide 6 (PA6) matrix and melt-blended nanocomposites [95]. Researchers melt-blended PA6 with Cloisite Na+, Cloisite 20A, and Cloisite 30B MMT nanoclays in a 30 mm twin-screw extruder and injection molding machine. Initially, PA6/Cloisite 20A MMT nanocomposites were manufactured at screw speeds of 100, 140, and 180 rpm. Here, the laminates were called as 20A100, 20A140, and 20A180. At the same speed, the neat PA6 matrices were melt-blended and the specimens were referred to as PA6100, PA6140, and PA6180. Second, the PA6/MMT nanocomposite was melt-blended with Cloisite Na+, Cloisite 20A, and Cloisite 30B at a screw speed of 140 rpm. The nanocomposites were named as Na + 140, 20A140, and 30B140, respectively. Surprisingly, the impact strength of the PA6/Cloisite 20A nanocomposite is lower than that of the pure matrix. This is because when fillers are added to the polymer matrix, microvoids are formed between the interfaces. The first three cycles have no effect on the impact strength of laminate 30B140. Similarly, the number of melt cycles has almost no effect on impact strength of Na + 140.

9. Interlaminar Shear Strength

Lu et al. tested the impact of 20 nm nano-SiO_2 by including in epoxy emulsifiers at the interfacial adhesion of carbon fiber-reinforced composites. The size of the carbon fibers used on this observation was approximately 7 μm and polyacrylonitrile (PAN) based. The various tests confirmed the interfacial interaction between carbon fiber and the modified epoxy. This phenomenon brought about the revised hydroxyl groups on the surface of carbon fibers after treating with nano-SiO_2 changed sizing. Consequently, the interlaminar shear strength of both unmodified and nano-SiO_2-modified sizing composite panels was superior to the unsized panels. The morphology test was carried out at the fractured surface of the ILSS specimen, and the outcomes affirmed that the nano-SiO_2-modified sizing shows excellent compact than the unmodified sizing [96]. With the assist of compression shear test, Santare et al. mentioned that 0.5 wt.% MWCNTs-loaded laminates yielded superior ILSS than unfilled laminates. The ILSS results lead to an increase in the shear strength of the matrix in a few instances or increased the strength of the fiber-matrix interface. Both shear punch and microdroplet tests absolutely concluded that the ILSS in particular trusted the fiber-matrix interface and did not rely on the shear strength of the matrix [97]. Likewise, the improved ILSS was detected for the CFRP nanocomposites with HNTs and CNFs toughened epoxy matrix by using a short-beam shear test [57, 92].

Kamae and Drzal advised a brand new approach for the motive of uniformly coating the CNTs to carbon fibers that permit the scalable fabrication of CNT-stuffed carbon fiber/epoxy nanocomposites [98]. The uniform coating between CNTs and carbon fibers is attained by dipping CFs into CNT/water suspension. Due to the repulsive force and attractive forces between CNTs and carbon fibers, an amazing dispersion rate was achieved. With the assist of single fiber fragmentation tests under shear loading, the shear strength was calculated. The test results show that the noticed improvement in interfacial shear strength was attained due to CNT-coated CFs. As shown in Table 4, the similar trend is portrayed in Table 4 showing the ILSS property for various nanofillers.

10. X-Ray Diffraction

Fuet al. synthesized the aircraft-grade epoxy-clay nanocomposite laminates and further examined the dispersion rate by using XRD. The nanofiller/polymer mixture was made with the aid of using a high-pressure mixing technique. Authors initially dispersed the nanoclay thoroughly in the acetone and later in the acetone epoxy solution. After that, the basal spacing between each nanoclay plate was tested by using the diffraction test. The test results revealed that the basal spacing of the nanoclay has increased from 2.37 nm to 3.22 nm due to the application of high shear and collision forces generated by mixing under high pressure. This large space between the individual platelet allows easy intercalation of acetone. As a result, the attractive force between the nanoclay layers is reduced. Therefore, the epoxy resins and curing agents easily entered into the nanoclay [100]. Dean et al. studied the dispersion rate of nanocomposite laminates made of organo-clay. The test results showed that with the increase of curing temperature and the increase of interlayer spacing, intercalated morphology with different interlayer gains was obtained. In addition, the rheological test showed that intergallery diffusion before curing has a decisive effect on the formation of exfoliation [101].

Initially, Singh et al., 2006, used the high shear mixing to obtain the uniform dispersion pattern between epoxy-nanoclay mixtures. The XRD results of fabricated epoxy/nanoclay laminates revealed that the complete exfoliation was occurring even to higher nanoclay loadings. Further, no outstanding peak appeared within the diffractograms for any samples produced by high shear mixer, and hence, complete exfoliation dispersion was ensured to all samples. But, a noticeable peak was obtained for 4 wt.% nanoclay loading samples dispersed by ultrasonication process [102].

Tolle and Anderson analyzed the role of preconditioning of organically modified clay in thermoset polymer during the fabrication process of laminates by using XRD and identified the sensitivity of exfoliation based on material conditions. The test results indicate the occurrence and extent of exfoliation morphology with various silicate preconditioning processes. In addition, due to the aging of the epoxy resin/nanoclay mixture and pretreatment, the delamination was obtained earlier and showed intercalation dispersion [103]. Krikorian and Pochan used polylactic acid resin (PLLA) and three organically modified MMTs, Cloisite 30B, Cloisite 25A, and Cloisite 15A, to synthesize nanocomposite laminates using an ultrasonicator, and then used a dryer to evaporate the solvent. Studies have shown that the

Table 4: ILSS property for various nanofillers.

Nanofiller	Dispersion status	ILSS property comments	Ref.
Cloisite 30B RXG 7000	1 wt.%, 3 wt.% 3 wt.%	Greater enhancement attained for 3 wt.% Cloisite 30B	[99]
Nano-silica	10 wt.%, 20 wt.%	12% greater reduction for 20 wt.% nano-silica-modified epoxy laminate	[89]
Nano-SiO_2	Unsized composites Unmodified sizing composites Nano-SiO_2-modified sizing composites	9% enhancement for unmodified sizing composites; 14% enhancement for nano-SiO_2-modified sizing composites	[96]
MWNT	0.5 wt.% unfunctionalized MWNT-modified epoxy 0.5 wt.% amino-functionalized MWNT-modified epoxy	41% increase than neat epoxy/glass fiber composites 61% increase than neat epoxy/glass fiber composites	[97]
Na + MMT clay	1, 3, 6, and 10% wt. of unmodified montmorillonite 1, 3, 6, and 10% wt. of organo-modified montmorillonite	ILSS reduced slightly and greater reduction for OMMT clay particles	[88]

scattering pattern depends upon basal spacing. In addition, due to the layered structure, the addition of nanoclay limits the PLLA. They also pointed out that adding more clay to the exposed matrix causes the material to become tougher [104]. However, Akbari and Bagheri achieved a combination of intercalated and exfoliated dispersions in polymer-layered silicate nanocomposites. Perform XRD testing to understand the dispersion pattern of epoxy-clay. From the XRD pattern, it was found that the significant improvement on $d_{(001)}$ spacing was attained to 5 wt.% MMT clay-epoxy matrix. The study further concluded that the interaction of clay-epoxy matrix decreases with the increasing clay content due to the presence of microvoids created by the rapid increase in viscosity. Therefore, the lower interaction of the mixture leads to a decrease in tensile strength [105]. Alamri and Low also based on the TEM test results of epoxy hybrid nanocomposites filled with cellulose fiber-reinforced clay platelets confirmed the same tendency of intercalation dispersion structure and exfoliation combination [106].

11. Chemical Analysis

Mansuri et al. made nanocomposites by grafting polystyrene on to Cloisite 20A. Infrared spectroscopy, thermogravimetric analysis (TGA), and dynamic thermal analysis are used to examine nanocomposite materials. Free radical polymerization is carried out during the synthesis process to form the homo-polymer into styrene, which results in the chemical grafting of polystyrene to the surface of the MMT clay and finally extraction from the grafted clay. The FTIR spectrum confirms the chemical grafting of polystyrene to the nanoclay surface. The test results show that polystyrene is chemically grafted to clay with a lower clay content [107].

Muhammad Sarfraz produced nanocomposites based on electroconductive structural polymers by adding carbon nanotubes (CNTs) to a Polybond matrix using a melt compounding method. In this research, Fourier transform infrared (FTIR) spectroscopy was used to examine the chemical structure of the nanocomposite. The results confirm the successful combination of CNT functional groups and multiple linking chains. Compared with pure laminates, nanocomposites have higher chemical resistance [108]. Similarly, You et al. used FTIR spectroscopy to chemically analyze nanoclay and carbon microfiber-loaded composites and to measure the chemical bonding of binders. During the manufacturing process, four different nanoclays and micromodifiers are added to the asphalt binder, namely, Nanomer I.44P, carbon micro-fiber, unmodified nanoclay, and polymer-modified nanoclay. The test results show that the addition of modifiers further improves the chemical stability and further delays the effects of aging and oxidation [109].

Ghorbel et al. used attenuated total reflectance/Fourier transform infrared (ATR/FTIR) spectroscopy to do interesting work on the chemical characterization of nanocomposite films. Nanocomposite films were produced using nano-whiskers made of cellulose (CNW) and nano-fibrillated cellulose (NFC) as the reinforcing phase and natural rubber latex as the matrix. In this research work, the ATR/FTIR method was used to examine the chemical bonds of natural rubber and the chemical bonds of nano-whiskers in the spectral range of 4000–600 cm^{-1}. The infrared spectroscopy test results witnessed that many vibrational modes were identified while adding cellulose nanoparticles (CNW/NFC) into the natural rubber matrix. Research also shows that the interface adhesion of NFC/natural rubber nanocomposite film is higher than that of CNW/natural rubber, due to the presence of residual lignin in NFC. It has also been observed that when the filler content is increased from 1% to 10%, with a significant effect on the vibration behavior [110].

12. Thermal Analysis

Altan et al. produced three sets of laminates, such as pure epoxy laminates, unfilled GFRP laminates, and Cloisite 25A-filled GFRP laminates. Dynamic mechanical analysis showed that the glass transition temperature of the nanoclay-filled GRP nanocomposite laminate was significantly higher than that of the other two laminates, due to the exfoliation properties of the nanoclay-loaded matrix [111]. Philippe et al. used a melting process to synthesize nanocomposite laminates from plasticized PLA and four different nanoclays (i.e., Cloisite Na +, Cloisite 25A, Cloisite 20A, and Cloisite

Table 5: Thermal properties of PI hybrid films (adapted from reference [113]).

FGS in PI (wt.%)	HDA-GS				AHB-GS			
	T_g (°C)	T_D^{ia} (°C)	wt_R^{600b} (%)	CTE^c (ppm/°C)	T_g (°C)	T_D^{ia} (°C)	wt_R^{600b} (%)	CTE^c(ppm/°C)
0 (pure PI)	260	539	85	61	260	539	85	61
3	242	499	88	58	251	530	86	53
5	236	468	87	55	239	471	85	51
10	210	439	85	46	221	443	85	41

30B). Thermal analysis of laminates was performed using differential scanning calorimetry and thermogravimetric analysis in an air stream heated at 20 K/min from 25 to 600°C. The test results show that the clay modified with bis(2-hydroxyethyl) methyl (hydrogenated tallow alkyl) ammonium cation has higher thermal stability [112]. In addition, it is also confirmed that as the clay content increases, the thermal decomposition of the resin is found to be delayed.

Tanoglu et al. described that the clay loading altered the thermal behavior of GFR clay/epoxy laminates. In addition, the study concluded that the addition of MMT clay significantly improved the fire resistance of the composite material [88]. Jin-Hae Chang's research focuses on combining polyimide with two different new functionalized graphene sheets (FGSs), namely, hexadecylamine-graphene sheets (HDA-GSs) and 4-amino-N-hexadecylbenzamide-graphene sheets (AHB-GSs) to synthesize mixed films by the solution intercalation method. The content of FGS filler in the hybrid film solution varies from 0 to 10% by weight. He then analyzed the effect of filler content material fabric on the nanocomposite to determine thermal performance. Extensive thermal studies have shown that adding a small amount of filler can significantly increase the coefficient of thermal expansion. Furthermore, as the filler content increases, the glass transition temperature and initial decomposition temperature of the hybrid film tend to decrease as shown in Table 5. The AHB-GS hybrids had predominant thermal properties than the HDA-GS nanocomposite films [113]. Krishnaswami et al. discussed the thermal insulation properties of aerogel/PA6 composites manufactured using a twin-screw extruder at two different speeds (65 rpm and 5 rpm) and a compression molding machine. Thermal analysis shows that low-speed laminates have the main thermal conductivity compared to high-speed laminates; however, the thermal conductivity of both nanocomposites is inferior to the virgin polymer. Furthermore, the thermal stability was improved for the polyamide 6/polypropylene blend with the inclusion of both Na-MMT and OMMT [114].

13. Conclusion

In recent years, nanocomposites have attracted many researchers based on the reports from Toyota and Giannelis research groups on improved performance. Nowadays, nanocomposites are popular in many industries in the manufacture of computer chips, food packaging, batteries, engine components, fuel tanks, impellers, and oxygen gas barriers. This overview outlines the impact of nanoparticles in the basic matrix on the production of nanocomposites and the factors that affect their performance.

Depending upon the diverse shapes, the nano-sized substances are used as particles (e.g., nanoparticles), sheets (e.g., nanoclay), fibers (e.g., carbon nanofibers), and tubes (e.g., carbon nanotubes). The addition of small nanofiller content material improved mechanical properties (like strength, modulus), thermal stability, interlaminar properties (like ILSS, fracture toughness), tribology properties (like the coefficient of friction), dielectric properties, and chemical resistance. Generally, the nanofillers contain a high aspect ratio and high surface-to-volume ratio. From the various researches carried out on different nanocomposites, it is determined that the nanofillers are included in the range of 0.5 to 10% by weight with the matrix. However, the superior properties can be acquired at a low filler content material of 0.5 wt.% to 5 wt.% dispersion with the base matrix.

The review showed that the mixture is dispersed at a high speed, and when using high-frequency dispersion equipment such as ultrasonicator, the nanofillers are agglomerated in high content loading due to the high aspect ratio and high surface-to-volume ratio. This leads to the formation of pores and weaker areas, and results in the formation and propagation of cracks. It was also found in this review that the viscosity of the clay matrix achieves the best improvement at low content due to good interfacial adhesion. In addition, improved viscosity leads to improved mechanical properties and thermal stability.

The review work elucidated that the dispersion rate of the clay matrix mixture can be divided into intercalation or exfoliation according to the d-spacing between each clay platelet. Generally, the d-spacing of nanoclay was increased appreciably at low clay content due to easy dispersion with matrix, so that enhanced surface binding was exhibited. Additionally, this work further investigated the dispersion of the curing agent into the nanoclay-epoxy blend and its effects. The study corroborates that the dispersion promotes the reaction with the matrix. Further, in some cases, the treatment of MMT nanoclay with the coupling agent brought a hydrophilic nature, which altered all properties considerably. The interlayer spacing varies according to the use of the swelling agent, whether it is a monomer or a polymer. This change finally ends in the attainment of intercalating or exfoliating smectite clay which inherently altered the properties. In most of the cases, the review work has analyzed the effect of nanofillers with the preparation techniques of composite laminates. The overall review

reveals that the inclusion of a less amount of nanofillers in polymers will be becoming more perfect in the property enhancement of composite materials.

Conflicts of Interest

The authors declare that there are no conflicts of interest or personal relationships that could have appeared to influence the work reported in this paper.

References

[1] R. L. Carlson, G. A. Kardomateas, and J. I. Craig, *Mechanics of Failure Mechanisms in Structures*, Springer, Berlin, Germany, 1st edition, 2012.

[2] T. Yokozeki, Y. Iwahori, and S. Ishiwata, "Matrix cracking behaviors in carbon fiber/epoxy laminates filled with cup-stacked carbon nanotubes (CSCNTs)," *Composites Part A: Applied Science and Manufacturing*, vol. 38, no. 3, pp. 917–924, 2007.

[3] S. Komarneni, "Feature article. Nanocomposites," *Journal of Materials Chemistry*, vol. 2, no. 12, pp. 1219–1930, 1992.

[4] E. P. Giannelis, "Polymer layered silicate nanocomposites," *Advanced Materials*, vol. 8, no. 1, pp. 29–35, 1996.

[5] M. S. Senthil Kumar, N. MohanaSundara Raju, P. S. Sampath, and L. S. JayaKumari, "Effects of nano-materials on polymer composites - an expatiate view," *Reviews on Advanced Materials Science*, vol. 38, pp. 40–54, 2014.

[6] R. Boujmal, C. A. Kakou, S. Nekhlaoui et al., "Alfa fibers/clay hybrid composites based on polypropylene: mechanical, thermal, and structural properties," *Journal of Thermoplastic Composite Materials*, vol. 31, no. 7, pp. 974–991, 2018.

[7] Y. Zhu, J. O. Iroh, R. Rajagopolan, A. Aydin, and V. Richard, "Optimizing the synthesis and thermal properties of conducting polymer–montmorillonite clay nanocomposites," *Energies*, vol. 15, pp. 1–18, 2022.

[8] K. P. Rajan, A. Al. Ghamdi, S. P. Thomas, A. Gopanna, and M. Chavali, "Dielectric analysis of polypropylene (PP) and polylactic acid (PLA) blends reinforced with halloysite nanotubes," *Journal of Thermoplastic Composite Materials*, vol. 31, no. 8, pp. 1042–1053, 2018.

[9] D. B. Miracle and S. L. Donaldson, *ASM Handbook Volume 21: Composites*, D. B. Miracle and S. L. Donaldson, Eds., ASM International, Materials Park, OH, USA, 2001.

[10] International Organization for Standardization, *Nanotechnologies - Vocabulary - Part 2:Nano-Objects (ISO/TS 80004-2: 2015)*, International Organization for Standardization, Switzerland, Geneva, 1st edition, 2015.

[11] M. Hosokawa, K. Nogi, M. Naito, and T. Yokoyama, *Nanoparticle Technology Handbook*, Elsevier Science, Oxford, UK, 2007.

[12] D. Schmidt, D. Shah, and E. P. Giannelis, "New advances in polymer/layered silicate nanocomposites," *Current Opinion in Solid State & Materials Science*, vol. 6, no. 3, pp. 205–212, 2002.

[13] D. Yang, H. Xu, and W. Yu, "Comparative study on the dielectric properties of three polyvinylidene fluoride nanocomposites incorporated with carbon filler," *Journal of Thermoplastic Composite Materials*, vol. 31, no. 8, pp. 1102–1111, 2018.

[14] S. Ghasemi, R. Behrooz, I. Ghasemi, R. S. Yassar, and F. Long, "Development of nanocellulose-reinforced PLA nanocomposite by using maleated PLA (PLA-g-MA)," *Journal of Thermoplastic Composite Materials*, vol. 31, no. 8, pp. 1090–1101, 2018.

[15] M. Alexandre and P. Dubois, "Polymer-layered Silicate Nanocomposites: preparation, properties and uses of a new class of materials," *Materials Science and Engineering: R: Reports*, vol. 28, no. 1–2, pp. 1–63, 2000.

[16] R. He, F. Niu F, and Q. Chang, "Tribological properties of PI-SiC nanocomposite prepared by hot dynamic compaction," *Journal of Thermoplastic Composite Materials*, vol. 31, no. 8, pp. 1066–1077, 2018.

[17] K. Müller, E. Bugnicourt, M. Latorre et al., "Review on the Processing and properties of polymer nanocomposites and nanocoatings and their applications in the packaging, automotive and solar energy fields," *Nanomaterials*, vol. 7, no. 74, pp. 1–47, 2017.

[18] J. Zhou, Z. Lin, H. Ren et al., "Layered intercalation materials," *Advanced Materials*, vol. 33, no. 25, pp. 1–23, 2021.

[19] J. Costa de Macedo Neto, N. Reis do Nascimento, R. Hoel Bello, L. Antonio de Verçosa, J. Evangelista Neto, and J. Carlos Martins da Costa and Francisco Rolando Valenzuela Diaz, "Kaolinite review: intercalation and production of polymer nanocomposites," *Engineered Science*, vol. 17, pp. 28–44, 2022.

[20] S. Kenig, *Processing of Polymer Nanocomposites*, pp. 1–497, Hanser Publications, Munich, Germany, 2019.

[21] S. Pavlidou and C. D. Papaspyrides, "A review on polymer– layered silicate nanocomposites," *Progress in Polymer Science*, vol. 33, no. 12, pp. 1119–1198, 2008.

[22] D. R. Paul and L. M. Robeson, "Polymer nanotechnology: nanocomposites," *Polymer*, vol. 49, no. 15, pp. 3187–3204, 2008.

[23] L. Mrah and R. Meghabar, "In situ polymerization of styrene–clay nanocomposites and their properties," *Polymer Bulletin*, vol. 78, pp. 3509–3526, 2021.

[24] C. IlPark, O. OkPark, J. GonLim, and H. Joon Kim, "The fabrication of syndiotactic polystyrene/organophilic clay nanocomposites and their properties," *Polymer*, vol. 42, no. 17, pp. 7465–7475, 2001.

[25] S. K. Zhade, S. K. Chokka, V. S. Babu, and K. V. Sai Srinadh, "A review on mechanical properties of epoxy-glass composites reinforced with nanoclay," in *Epoxy-Based Composites*, S. Chelladurai, Ed., Intech Open, London, UK, 2022.

[26] S. S. Chee, M. Jawaid, O. Y. Alothman, and H. Fouad, "Effects of nanoclay on mechanical and dynamic mechanical properties of bamboo/kenaf reinforced epoxy hybrid composites," *Polymers*, vol. 13, no. 3, pp. 1–17, 2021.

[27] H. Wang, A. Sun, X. Qi, Y. Dong, and B. Fan, "Experimental and analytical investigations on tribological properties of PTFE/AP composites," *Polymers*, vol. 13, no. 24, pp. 1–14, 2021.

[28] B. Anitha, B. V. Vibitha, P. S. P. Jyothi, and J. N. Tharayi, "Structural and morphological studies of conducting polymer nanocomposites," *AIP Conference Proceedings*, vol. 2287, no. 1, pp. 1–4, 2020.

[29] A. Dorigato and A. Pegorettia, "Nanocomposite and its morphological characterization -review," *IOP Conference Series: Materials Science and Engineering*, vol. 640, pp. 1–9, 2019.

[30] K. Mohan Babu and M. Mettilda, "Morphological studies on renewable castor oil-based nanocomposites with modified clay and MWCNTs as fillers," *Polymers and Polymer Composites*, vol. 29, no. 1 – 8, 2020.

[31] D. L. Shi, X. Q. Feng, Y. Y. Huang, K.-C. Hwang, and H. Gao, "The effect of nanotube waviness and agglomeration on the

elastic property of carbon nanotube-reinforced composites," *Journal of Engineering Materials and Technology*, vol. 126, no. 3, pp. 250–257, 2004.

[32] Y. Wang, J. W. Shan, and G. J. Weng, "Percolation threshold and electrical conductivity of graphene-based nanocomposites with filler agglomeration and interfacial tunneling," *Journal of Applied Physics*, vol. 118, pp. 1–10, Article ID 065101, 2015.

[33] S. Gong, Z. H. Zhu, and S. A. Meguid, "Carbon nanotube agglomeration effect on piezoresistivity of polymer nanocomposites," *Polymer*, vol. 55, no. 21, pp. 5488–5499, 2014.

[34] J. Pan and L. Bian, "Coefficients of nonlinear thermal expansion for fiber-reinforced composites," *Acta Mechanica*, vol. 228, no. 12, pp. 4341–4351, 2017.

[35] P. Barai and G. J. Weng, "A theory of plasticity for carbon nanotube reinforced composites," *International Journal of Plasticity*, vol. 27, no. 4, pp. 539–559, 2011.

[36] X.-Y. Ji, Y. Cao, and X.-Q. Feng, "Micromechanics prediction of the effective elastic moduli of graphene sheet-reinforced polymer nanocomposites," *Modelling and Simulation in Materials Science and Engineering*, vol. 18, no. 4, pp. 1–16, Article ID 045005, 2010.

[37] E. W. Tiedje and P. Guo, "Modeling the influence of particulate geometry on the thermal conductivity of composites," *Journal of Materials Science*, vol. 49, no. 16, pp. 5586–5597, 2014.

[38] A. Tessema, D. Zhao, J. Moll et al., "Effect of filler loading, geometry, dispersion and temperature on thermal conductivity of polymer nanocomposites," *Polymer Testing*, vol. 57, pp. 101–106, 2017.

[39] M. S. Senthil Kumar, N. Mohana Sundara Raju, P. S. Sampath, and U. Vivek, "Tribological analysis of nano clay/epoxy/glass fiber by using Taguchi's technique," *Materials & Design*, vol. 70, pp. 1–9, 2015.

[40] M. S. Senthil Kumar, A. Adugna, K. Balasundaram, and A. Ashok Kumar, "Vibration analysis of nanoclay reinforced glass fiber/epoxy nanocomposite," *Journal of Recent Research in Engineering and Technology*, vol. 4, no. 5, pp. 1–6, 2017.

[41] C. M. Manjunatha, R. Bojja, N. Jagannathan, A. J. Kinloch, and A. C. Taylor, "Enhanced fatigue behavior of a glass fiber reinforced hybrid particles modified epoxy nanocomposite under WISPERX spectrum load sequence," *International Journal of Fatigue*, vol. 54, pp. 25–31, 2013.

[42] C. M. Manjunatha, N. Jagannathan, K. Padmalatha, A. C. Taylor, and A. J. Kinloch, "The effect of micron-rubber and nano-silica particles on the fatigue crack growth behavior of an epoxy polymer," *International Journal of Nanoscience*, vol. 10, no. 4, pp. 1095–1099, 2011.

[43] G. Hug, P. Thévenet, J. Fitoussi, and D. Baptiste, "Effect of the loading rate on mode I interlaminar fracture toughness of laminated composites," *Engineering Fracture Mechanics*, vol. 73, pp. 2456–2462, 2006.

[44] M. H. Woldemariam, G. Belingardi, E. G. Koricho, and D. T. Reda, "Effects of nanomaterials and particles on mechanical properties and fracture toughness of composite materials: a short review," *AIMS Materials Science*, vol. 6, no. 5, pp. 1191–1212, 2019.

[45] S. Mazumdar, *Composites Manufacturing, Materials, Product and Process Engineering*, CRC Press, Boca Raton, FL, USA, 1st edition, 2001.

[46] F. H. Su, Z. Z. Zhang, and W. M. Liu, "Tribological and mechanical properties of Nomex fabric composites filled with polyfluo 150 wax and nano-SiO_2," *Composites Science and Technology*, vol. 67, pp. 102–110, 2007.

[47] Z. Z. Wang, P. Gu, Z. Zhang, L. Gu, and Y. Z. Xu, "Mechanical and tribological behavior of epoxy/silica nanocomposites at the micro/nanoscale," *Tribology Letters*, vol. 42, pp. 185–191, 2011.

[48] Y. Kang, X. Chen, S. Song, L. Yu, and P. Zhang, "Friction and wear behavior of nanosilica-filled epoxy resin composite coatings," *Applied Surface Science*, vol. 258, pp. 6384–6390, 2012.

[49] S. Thakur and S. R. Chauhan, "Friction and sliding wear characteristics study of submicron size cenosphere particles filled vinylester composites using Taguchi design of experimental technique," *Journal of Composite Materials*, vol. 48, no. 23, pp. 1–12, 2013.

[50] B. P. Chang, H. M. Akil, M. G. Affendy, A. Khan, and R. Bt Md Nasir, "Comparative study of wear performance of particulate and fiber-reinforced nano-ZnO/ultra-high molecular weight polyethylene hybrid composites using response surface methodology," *Materials & Design*, vol. 63, pp. 805–819, 2014.

[51] B. P. Chang, H. M. Akil, R. B. M. Nasir, I. M. C. C. D. Bandara, and S. Rajapakse, "The effect of ZnO nanoparticles on the mechanical, tribological and antibacterial properties of ultra-high molecular weight polyethylene," *Journal of Reinforced Plastics and Composites*, vol. 33, no. 7, pp. 1–13, 2014.

[52] M. Garcia, M. D. Rooij, L. Winnubst, W. E. Van Zyl, and H. Verweij, "Friction and wear studies on nylon-6/SiO_2 nanocomposites," *Journal of Applied Polymer Science*, vol. 92, pp. 1855–1862, 2004.

[53] B. Qi, Q. X. Zhang, M. Bannister, and Y.-W. Mai, "Investigation of the mechanical properties of DGEBA-based epoxy resin with nanoclay additives," *Composite Structures*, vol. 75, pp. 514–519, 2006.

[54] T. Yokozeki, Y. Iwahori, S. Ishiwata, and K. Enomoto, "Mechanical properties of CFRP laminates manufactured from unidirectional prepregs using CSCNT-dispersed epoxy," *Composites Part A: Applied Science and Manufacturing*, vol. 38, no. 10, pp. 2121–2130, 2007.

[55] W. Chen, H. Shen, M. L. Auad, C. Huang, and S. Nutta, "Basalt fiber–epoxy laminates with functionalized multiwalled carbon nanotubes," *Composites Part A: Applied Science and Manufacturing*, vol. 40, no. 8, pp. 1082–1089, 2009.

[56] F. Nanni, B. L. Mayoral, F. Madau, G. Montesperelli, and T. Mc Nally, "Effect of MWCNT alignment on mechanical and selfmonitoring properties of extruded PET–MWCNT nanocomposites," *Composites Science and Technology*, vol. 72, no. 10, pp. 1140–1146, 2012.

[57] X. Kornmann, M. Rees, Y. Thomann, A. Necola, M. Barbezat, and R. Thomann, "Epoxy-layered silicate nanocomposites as matrix in glass fibre-reinforced composites," *Composites Science and Technology*, vol. 65, no. 14, pp. 2259–2268, 2005.

[58] R. Pal, H. N. H. Murthy, K. S. Rai, and M. Krishna, "Influence of organo modified nanoclay on the mechanical behaviour of vinylester/glass nanocomposites," *International Journal of ChemTech Research*, vol. 6, pp. 916–928, 2014.

[59] A. Dorigato and A. Pegorettia, "Development and thermomechanical behavior of nanocomposite epoxy adhesives," *Polymers for Advanced Technologies*, vol. 23, pp. 660–668, 2011.

[60] L. Aktas, Y. K. Hamidi, and M. C. Altan, "Dispersion characterization of nanoclay in molded epoxy disks by combined image analysis and wavelength dispersive spectrometry," *Journal of Engineering Materials and Technology*, vol. 130, pp. 1–9, 2005.

[61] K. Panneerselvam and J. Daniel, "An experimental investigation on polymeric nanocomposite material," in *Proceedings of the All India Manufacturing Technology, Design and Research Conference (AIMTDR 2014)*, p. 298, IIT Guwahati, Guwahati, India, December 2014.

[62] Q. Zhang, J. Liu, R. Sager, L. Dai, and J. Baur, "Hierarchical composites of carbon nanotubes on carbon fiber: influence of growth condition on fiber tensile properties," *Composites Science and Technology*, vol. 69, no. 5, pp. 594–601, 2009.

[63] H. He, K. Li, J. Wang, G. Sun, Y. Li, and J. Wan, "Study on thermal and mechanical properties of nano-calcium carbonate/epoxy Composites," *Materials & Design*, vol. 32, no. 8–9, pp. 4521–4527, 2011.

[64] D. R. Bortz, C. Merino, and I. Martin-Gullon, "Mechanical characterization of hierarchical carbon fiber/nanofiber composite laminates," *Composites Part A: Applied Science and Manufacturing*, vol. 42, no. 11, pp. 1584–1591, 2011.

[65] N. Phonthammachai, X. Li, S. Wong, H. Chia, W. Weei Tjiu, and C. He, "Fabrication of CFRP from high performance clay/epoxy nanocomposite: preparation conditions, thermal–mechanical properties and interlaminar fracture characteristics," *Composites Part A: Applied Science and Manufacturing*, vol. 42, no. 8, pp. 881–887, 2011.

[66] L. B. Manfredi, H. D. Santis, and A. Vázquez, "Influence of the addition of montmorillonite to the matrix of unidirectional glass fibre/epoxy composites on their mechanical and water absorption properties," *Composites Part A: Applied Science and Manufacturing*, vol. 39, no. 11, pp. 1726–1731, 2008.

[67] M. K. Hossain, M. E. Hossain, M. V. Hosur, and S. Jeelani, "Flexural and compression response of woven E-glass/polyester–CNF nanophased composites," *Composites Part A: Applied Science and Manufacturing*, vol. 42, no. 11, pp. 1774–1782, 2011.

[68] B. Sharma, S. Mahajan, R. Chhibber, and R. Mehta, "Glass fiber reinforced polymer-clay nanocomposites: processing, structure and hygrothermal effects on mechanical properties," *Procedia Chemistry*, vol. 4, pp. 39–46, 2012.

[69] J. Li and R. Luo, "Study of the mechanical properties of carbon nanofiber reinforced carbon/carbon composites," *Composites Part A: Applied Science and Manufacturing*, vol. 39, no. 11, pp. 1700–1704, 2008.

[70] M. Madhoushi, A. Chavooshi, A. Ashori, M. P. Ansell, and A. Shakeri, "Properties of wood plastic composite panels made from waste sanding dusts and nanoclay," *Journal of Composite Materials*, vol. 48, no. 14, pp. 1–9, 2014.

[71] B. Suresha, B. N. Ravi Kumar, M. Venkataramareddy, and T. Jayarajua, "Role of micro/nano fillers on mechanical and tribological properties of polyamide66/polypropylene composites," *Materials & Design*, vol. 31, no. 4, pp. 1993–2000, 2010.

[72] J. Zhang, T. Lin, and X. Wang, "Electrospun nanofibre toughened carbon/epoxy composites: effects of polyetherketone cardo (PEK-C) nanofibre diameter and interlayer thickness," *Composites Science and Technology*, vol. 70, no. 11, pp. 1660–1666, 2010.

[73] Y. Xu and S. V. Hoa, "Mechanical properties of carbon fiber reinforced epoxy/clay Nanocomposites," *Composites Science and Technology*, vol. 68, no. 3-4, pp. 854–861, 2008.

[74] A. J. Rodriguez, M. E. Guzman, C. S. Lim, and B. Minaie, "Mechanical properties of carbon nanofiber/fiber-reinforced hierarchical polymer composites manufactured with multiscale-reinforcement fabrics," *Carbon*, vol. 49, no. 3, pp. 937–948, 2011.

[75] M. F. Uddin and C. T. Sun, "Strength of unidirectional glass/epoxy composite with silica nanoparticle-enhanced matrix," *Composites Science and Technology*, vol. 68, no. 7–8, pp. 1637–1643, 2008.

[76] C. M. Manjunatha, A. C. Taylor, A. J. Kinloch, and S. Sprenger, "The tensile fatigue behavior of a silica nanoparticle modified glass fibre reinforced epoxy composite," *Composites Science and Technology*, vol. 70, no. 1, pp. 193–199, 2010.

[77] A. K. Subramaniyan and C. T. Sun, "Enhancing compressive strength of unidirectional polymeric composites using nanoclay," *Composites Part A: Applied Science and Manufacturing*, vol. 37, no. 12, pp. 2257–2268, 2006.

[78] Y. Iwahori, S. Ishiwata, T. Sumizawa, and T. Ishikawa, "Mechanical properties improvements in two-phase and three-phase composites using carbon nano-fiber dispersed resin," *Composites Part A: Applied Science and Manufacturing*, vol. 36, no. 10, pp. 1430–1439, 2005.

[79] S. Arun, M. Maharana, and S. Kanagaraj, "Optimizing the processing conditions for the reinforcement of epoxy resin by multiwalled carbon nanotubes," *Journal of Nanotechnology*, vol. 2013, Article ID 634726, 6 pages, 2013.

[80] A. Jumahat, C. Soutis, J. Mahmud, and N. Ahmad, "Compressive properties of nanoclay/epoxy nanocomposites. International symposium on robotics and intelligent sensors," *Procedia Engineering*, vol. 41, pp. 1607–1613, 2012.

[81] L. Böger, J. Sumfleth, H. Hedemann, and K. Schulte, "Improvement of fatigue life by incorporation of nanoparticles in glass fiber reinforced epoxy," *Composites Part A: Applied Science and Manufacturing*, vol. 41, no. 10, pp. 1419–1424, 2010.

[82] Y. Zhou, F. Pervin, S. Jeelani, and P. K. Mallick, "Improvement in mechanical properties of carbon fabric–epoxy composite using carbon nanofibers," *Journal of Materials Processing Technology*, vol. 198, no. 1–3, pp. 445–453, 2008.

[83] C. M. Manjunatha, S. Sprenger, A. C. Taylor, and A. J. Kinloch, "The tensile fatigue behavior of a glass-fiber reinforced plastic composite using a hybrid toughened epoxy matrix," *Journal of Composite Materials*, vol. 44, no. 17, pp. 2095–2109, 2010.

[84] C. M. Manjunatha, N. Jagannathan, K. Padmalatha, A. J. Kinloch, and A. C. Taylor, "Improved variable-amplitude fatigue behavior of a glass-fiber-reinforced hybrid-toughened epoxy composite," *Journal of Reinforced Plastics and Composites*, vol. 30, no. 21, pp. 1783–1793, 2011.

[85] B. C. Kim, S. W. Park, and D. G. Lee, "Fracture toughness of the nanoparticle reinforced epoxy composites," *Composite Structures*, vol. 86, no. 1–3, pp. 69–77, 2008.

[86] V. Morote-Martínez, R. Torregrosa-Coque, and J. M. Martín-Martínez, "Addition of unmodified nanoclay to improve the performance of unsaturated polyester resin coating on natural stone," *International Journal of Adhesion and Adhesives*, vol. 31, no. 3, pp. 154–163, 2011.

[87] N. A. Siddiqui, R. S. C. Woo, J. K. Kim, C. C. K. Leung, and A. Munir, "Mode I interlaminar fracture behavior and mechanical properties of CFRPs with nanoclay-filled epoxy matrix," *Composites Part A: Applied Science and Manufacturing*, vol. 38, no. 2, pp. 449–460, 2007.

[88] E. Bozkurt, E. Kaya, and M. Tanoglu, "Mechanical and thermal behavior of non-crimp glass fiber reinforced layered clay/epoxy nanocomposites," *Composites Science and Technology*, vol. 67, no. 15–16, pp. 3394–3403, 2007.

[89] Y. Tang, L. Ye, D. Zhang, and S. Deng, "Characterization of transverse tensile interlaminar shear and interlaminate

fracture in CF/EP laminates with 10 wt.% and 20 wt.% silica nanoparticles in matrix resins," *Composites Part A: Applied Science and Manufacturing*, vol. 42, no. 12, pp. 1943–1950, 2011.

[90] D. C. Davis and B. D. Whelan, "An experimental study of interlaminar shear fracture toughness of a nanotube reinforced composite," *Composites Part B: Engineering*, vol. 42, no. 1, pp. 105–116, 2011.

[91] Y. Ye, H. Chen, J. Wu, and C. M. Chan, "Interlaminar properties of carbon fiber composites with halloysite nanotube-toughened epoxy matrix," *Composites Science and Technology*, vol. 71, no. 5, pp. 717–723, 2011.

[92] V. Kostopoulos, P. Tsotra, P. Karapappas et al., "Mode I interlaminar fracture of CNF or/and PZT doped CFRPs via acoustic emission monitoring," *Composites Science and Technology*, vol. 67, no. 5, pp. 822–828, 2007.

[93] X. F. Yao, D. Zhou, and H. Y. Yeh, "Macro/microscopic fracture characterizations of SiO_2/epoxy nanocomposites," *Aerospace Science and Technology*, vol. 12, no. 3, pp. 223–230, 2008.

[94] D. Zhang, L. Ye, D. Wang, Y. Tang, S. Mustapha, and Y. Chen, "Assessment of transverse impact damage in GF/EP laminates of conductive nanoparicles using electrical resistivity tomography," *Composites Part A: Applied Science and Manufacturing*, vol. 43, no. 9, pp. 1587–1598, 2011.

[95] J. H. Lin, C. W. Lin, C. H. Huang, C.-L. Huang, and C.-W. Lou, "Manufacturing technique and mechanical properties of plastic nanocomposite," *Composites Part B: Engineering*, vol. 44, no. 1, pp. 34–39, 2013.

[96] Y. Yang, C. X. Lu, X. L. Su, and G. P. Wu, "Effect of nano SiO_2 modified emulsion sizing on the interfacies adhesion of carbon filers reinforced composites," *Materials Letters*, vol. 61, no. 17, pp. 3601–3604, 2007.

[97] V. C. S. Chandrasekaran, S. G. Advani, and M. H. Santare, "Influence of resin properties on interlaminar shear strength of glass/epoxy/MWNT hybrid composites," *Composites Part A: Applied Science and Manufacturing*, vol. 42, no. 8, pp. 1007–1016, 2011.

[98] T. Kamae and L. T. Drzal, "Carbon fiber/epoxy composite property enhancement through incorporation of carbon nanotubes at the fiber–matrix interphase – Part I: the development of carbon nanotube coated carbon fibers and the evaluation of their adhesion," *Composites Part A: Applied Science and Manufacturing*, vol. 43, no. 9, pp. 1569–1577, 2012.

[99] M. Quaresimin, M. Salviato, and M. Zappalorto, "Fracture and interlaminar properties of clay-modified epoxiesand their glass reinforced laminates," *Engineering Fracture Mechanics*, vol. 81, pp. 80–93, 2012.

[100] S. Fu, Z. Sun, P. Huang, Y. Li, and N. Hu, "Some basic aspects of polymer nanocomposites: a critical review," *Nano Materials Science*, vol. 1, no. 1, pp. 2–30, 2019.

[101] D. Dean, R. Walker, M. Theodore, E. Hampton, and E. Nyairo, "Chemorheology and properties of epoxy/layered silicate nanocomposites," *Polymer*, vol. 46, no. 9, pp. 3014–3021, 2005.

[102] S. C. Zunjarrao, R. Sriraman, and R. P. Singh, "Effect of processing parameters and clay volume fraction on the mechanical properties of epoxy-clay nanocomposites," *Journal of Materials Science*, vol. 41, no. 8, pp. 2219–2228, 2006.

[103] T. B. Tolle and D. P. Anderson, "The role of preconditioning on morphology development in layered silicate thermoset nanocomposites," *Journal of Applied Polymer Science*, vol. 91, no. 1, pp. 89–100, 2004.

[104] V. Krikorian and D. J. Pochan, "Poly (L-Lactic Acid)/layered silicate nanocomposite: fabrication, characterization and properties," *Chemistry of Materials*, vol. 15, no. 22, pp. 4317–4324, 2003.

[105] B. Akbari and R. Bagheri, "Deformation mechanism of epoxy/clay nanocomposite," *European Polymer Journal*, vol. 43, no. 3, pp. 782–788, 2007.

[106] H. Alamri and I. M. Low, "Effect of water absorption on the mechanical properties of nanoclay filled recycled cellulose fibre reinforced epoxy hybrid nanocomposites," *Composites Part A: Applied Science and Manufacturing*, vol. 44, pp. 23–31, 2013.

[107] Y. Mansoori, K. Roojaei, M. R. Zamanloo, and G. Imanzadeh, "Polymer-clay nanocomposites: chemical grafting of polystyrene onto Cloisite 20A," *Chinese Journal of Polymer Science*, vol. 30, pp. 815–823, 2012.

[108] M. Sarfraz, "Upgrading electrical, mechanical, and chemical properties of CNTs/polybond nanocomposites: pursuit of electroconductive structural polymer nanocomplexes," *International Journal of Polymer Science*, vol. 2016, Article ID 2396817, 8 pages, 2016.

[109] H. Yao, Z. You, Li L. Liang et al., "Rheological properties and chemical analysis of nanoclay and carbon microfiber modified asphalt with Fourier transform infrared spectroscopy," *Construction and Building Materials*, vol. 38, pp. 327–337, 2013.

[110] F. Agrebi, N. Ghorbel, S. Bresson, O. Abbas, and A. Kallel, "Study of nanocomposites based on cellulose nanoparticles and natural rubber latex by ATR/FTIR spectroscopy: the impact of reinforcement," *Polymer Composites*, vol. 40, no. 5, pp. 2076–2087, 2019.

[111] L. Aktas, Y. K. Hamidi, and M. C. Altan, "Characterisation of nanoclay dispersion in resin transfer moulded glass/nanoclay/epoxy composites," *Plastics, Rubber and Composites*, vol. 33, no. 6, pp. 267–272, 2004.

[112] M. A. Paul, M. Alexandre, P. Degée, C. Henrist, A. Rulmont, and P. Dubois, "New nanocomposite materials based on plasticized poly(L-lactide) and organo-modified montmorillonites: thermal and morphological study," *Polymer*, vol. 44, no. 2, pp. 443–450, 2003.

[113] J. H. Chang, "Polyimide nanocomposites with functionalized graphene sheets: thermal property, morphology, gas permeation, and electroconductivity," *Journal of Thermoplastic Composite Materials*, vol. 31, no. 6, pp. 837–861, 2018.

[114] S. Krishnaswamy, L. Tinsley, V. Marchante, S. Addepalli, Z. Huang, and H. Abhyankar, "Effect of extrusion and compression moulding on the thermal properties of nylon-6/silica aerogel composites," *Journal of Thermoplastic Composite Materials*, vol. 31, no. 7, pp. 992–1009, 2018.